

Critical temperature for mound formation in molecular-beam epitaxy

Jacques G. Amar and Fereydoon Family

Department of Physics, Emory University, Atlanta, Georgia 30322

(Received 22 May 1996)

The results of an analytic calculation of the surface current and selected mound angle as a function of the Ehrlich-Schwoebel step barrier E_B and substrate temperature T are presented for a model of epitaxial growth on bcc(100) and fcc(100) surfaces. Depending on the sign of E_B and the magnitude of the prefactor for diffusion over a step, various scenarios are possible, including the existence of a critical temperature T_c for mound formation *above* which (for a positive step barrier) or *below* which (for a negative step barrier) quasi-layer-by-layer growth will be observed. For the case of Fe/Fe(100) deposition our calculation implies an upper bound for T_c which is consistent with experiment. The weak parameter dependence of our estimates for the mound angle confirms and explains the good agreement found in previous estimates assuming different values of the step barrier. We also clarify the transition to layer-by-layer growth at low and high temperature including the effect of a finite diffusion length on reentrant behavior at low temperature. [S0163-1829(96)04343-3]

I. INTRODUCTION

The role of the Ehrlich-Schwoebel step barrier¹⁻⁴ (defined as the difference between the energy barrier for an adatom to hop from a terrace to the layer below and the energy barrier for diffusion on a flat terrace) in determining the surface morphology in epitaxial growth has been the subject of a large amount of recent experimental and theoretical work. In particular, the existence of a barrier to interlayer diffusion has been shown to lead to a morphological instability^{5,6} and the formation of "mounds," ripples, or facets which coarsen with time.⁶⁻¹³ For example, recent experiments on Fe/Fe(100) deposition at room temperature¹¹ have demonstrated the formation of mound structures with a selected "magic" angle of approximately 13°. In addition, recent experiments on Fe/MgO(001) deposition at $T \approx 180$ °C (Ref. 12) have led to pyramid formation in which [012] facets were observed. Similarly, recent experiments on Cu/Cu(100) deposition indicate the formation of low-angle [113] facets at $T = 160$ K and [115] facets at 200 K. Low-angle mound formation has also been observed in Ge/Ge(100),¹³ GaAs/GaAs(100),⁶ and possibly in Ag/Ag(100).¹⁴

Recently, we have shown^{15,16} that for deposition on metal fcc(100) and bcc(100) surfaces, the presence of a selected mound angle may be explained as a result of the competition between an upward surface current due to the reflection of adatoms from descending steps (due to the step barrier) and the effects of crystal geometry, which lead to a downward (negative) current due to atoms deposited near step edges. The value of the selected angle corresponds to the slope for which the surface current is zero. In particular, in recent kinetic Monte Carlo simulations of Fe/Fe(100) growth at room temperature¹⁵⁻¹⁷ good agreement for the selected mound angle and mound coarsening behavior with experiment has been found, using reasonable estimates for the value of the interlayer step barrier for Fe/Fe(100). In addition, an approximate analytical calculation of the surface current assuming an infinitely large step barrier was also carried out^{15,16} and found to give a reasonable prediction for the

selected mound angle for Fe/Fe(100) at room temperature. These results appear to confirm the scenario of a kinetically determined mound angle based on a competition between upward and downward currents.

We note, however, that there may be situations in which the step barrier E_B is not present or is relatively weak, and in this case mound formation may not occur. For example, simulations indicate that for the case of no step barrier ($E_B = 0$) mound formation does not occur.¹⁶ In addition, recent experiments⁶ on GaAs(100) deposition at 555 °C demonstrate the existence of low-angle (approximately 1.5°) mounds, suggesting that if the angle selection is due to a similar kinetic mechanism in this case, then the step-barrier involved is relatively weak. Thus, two general questions emerge. (i) Is there a critical temperature above which mound formation no longer occurs? (ii) What is the dependence of the mound angle on temperature (for a given value of the step barrier) or more precisely on the ratio $E_B/k_B T$? Here we try to answer these questions by extending our previous calculation of the surface current and selected mound angle on a (100) surface for an infinite barrier¹⁶ to the case of a finite step barrier.

II. MODEL

As in Refs. 15 and 16 we consider a quasi-one-dimensional model consisting of a regular stepped bcc(100) or fcc(100) surface with infinitely long straight steps along the [001] direction (see Fig. 1) with slope m and terrace length $l = 1/m$ (in units of 1/2 the next-nearest-neighbor distance) where $l = 2j + 1$ and j is the number of exposed rows in each (100) terrace. Assuming that steps are relatively straight due to edge diffusion [as is the case for Fe/Fe(100)] such a model is appropriate in the asymptotic (late-time) limit since in this limit the mound size is significantly larger than the terrace size. With a slight modification of the crystal geometry, a similar model may also be appropriate in the case of the one-dimensional ripple structures observed in GaAs(100) deposition. We note that the notation used here

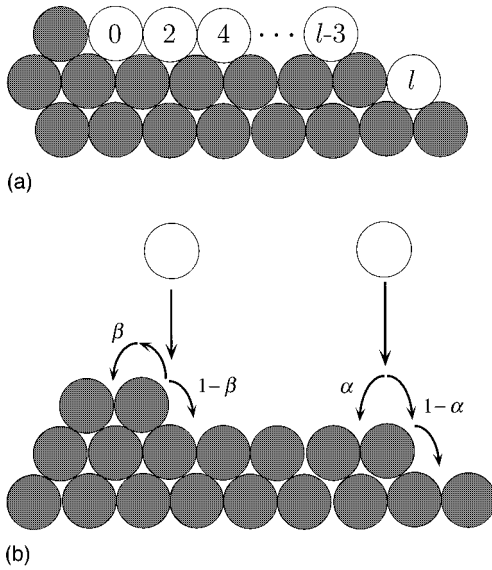


FIG. 1. Diagram showing stepped bcc (100) surface with slope m (terrace width $l=1/m$) and straight step edges along the (001) axis (side view). (a) Even sites correspond to fourfold hollow sites on terrace. Sites labeled 0 and l are step-attachment sites. (b) Arrows show probabilities of upward and downward funneling after deposition at a step.

refers to a bcc(100) geometry [as for Fe(100)] and in this case the tilted surface considered here corresponds to a $[10\bar{1}]$ facet. However, these calculations also apply to deposition on a fcc(100) surface. In particular, for this case the stepped surface corresponds to a $[\bar{1}1\bar{1}]$ facet, while the actual value of the selected slope is $\sqrt{2}$ times larger due to the difference in the relative spacing between layers.

For a given slope m , the surface current per particle (J) may be estimated by multiplying the probability m that an atom will be deposited at a given site by the average (signed) distance traveled before incorporation at an ascending or descending step. For simplicity, we assume irreversible attachment at ascending steps (site 0 or l in Fig. 1). This is appropriate for a variety of systems over a range of temperatures, although at high enough temperatures detachment from step edges may need to be taken into account. As in previous work,^{15,16} we assume that freshly deposited atoms may only be incorporated at epitaxial growth sites so that atoms which do not land on fourfold hollow sites, must “cascade” to the nearest fourfold hollow site before diffusing and being incorporated into the surface.

The selected slope m_0 is then determined by finding the value of the slope for which the surface current is zero.^{18–21} In the usual downward funneling models^{15,16,23,24} one assumes that particles which land at the edge of a step (site $l-2$ in Fig. 1) will go with equal probability to the nearest fourfold hollow sites on the upper or lower terraces. More generally, an adatom deposited at such a site might hop with different probabilities to the upper and lower terraces due to various effects at a step edge. Therefore, we consider the general case in which a particle landing at the edge of a step (site $l-2$) will “cascade” to the fourfold hollow site on the upper terrace with probability α and to the lower terrace attachment site with probability $1-\alpha$ [see Fig. 1(b)]. Similarly, in the usual downward funneling models one assumes

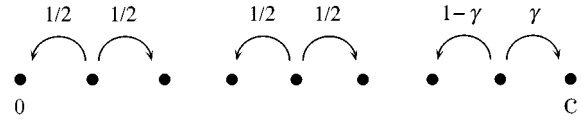


FIG. 2. Diagram showing random walk (on sites corresponding to fourfold hollow terrace sites in Fig. 1) between absorbing sites at 0 and c .

that a particle landing at site $l-1$ will cascade with probability 1 to the attachment site 0 on the lower terrace. However, for generality we consider the case in which such a particle “cascades” to the lower terrace attachment site with probability $1-\beta$ and to the upper terrace with probability β [see Fig. 1(b)]. For comparison with Fe/Fe(100) deposition at room temperature, it appears that the simplest assumption ($\alpha=1/2$ and $\beta=0$) is most appropriate.

III. CALCULATION OF SURFACE CURRENT AND MOUND ANGLE

The total surface current J may be divided into two contributions (see Fig. 1). The first contribution (J_1) comes from processes which lead to immediate attachment of a freshly deposited adatom at a step edge (site 0 or l). These include deposition at site $l-2$ followed by a cascade to the right by two units with probability $1-\alpha$, deposition at site $l-1$ followed by a cascade to the right with probability $1-\beta$, and deposition at site 1 followed by a cascade to the left with probability $1/2$. Summing, we obtain $J_1=(2\alpha+\beta-5/2)m$.

The second contribution to the surface current (J_2) corresponds to those processes in which diffusion on the terrace takes place before attachment to an ascending or descending step. In particular, particles are assumed to diffuse randomly to the right or to the left on fourfold hollow terrace sites [i.e., even sites $2i$ with $i=1$ to $(l-5)/2$] away from a step edge and be absorbed at the “step-attachment sites” 0 or l . However, at the edge of a terrace [site $(l-3)$ in Fig. 1], due to the step barrier, the probability of a hop to the right is given by $\gamma=(\nu_B/\nu_0)e^{-E_B/k_B T}/[1+(\nu_B/\nu_0)e^{-E_B/k_B T}]$, where ν_B/ν_0 is the ratio of the frequency factors for hopping to the right versus hopping to the left at the step edge, and the probability of a hop to the left is given by $1-\gamma$. This can be mapped to a random walk between two absorbing barriers at 0 and c as shown in Fig. 2, in which walkers at sites i with $1\leq i\leq c-2$ (corresponding to adatoms at sites $2i$ in Fig. 2) hop randomly to the right or to the left with probability $1/2$, while a walker at site $c-1$ hops to the right (left) with probability γ ($1-\gamma$) and where $c=(l-1)/2$. This leads to the following expression for J_2 :

$$J_2=(\alpha-1/2)m(lP_{(l-3)/2}-2)+\beta m(lP_{(l-3)/2}-1) + 2m \sum_{i=1}^{(l-3)/2} [2iP_i-(1-P_i)(l-2i)], \quad (1)$$

where P_i is the probability that a particle deposited at site $2i$ will attach at site 0 (e.g., the upper step), the factor of 2 in front of the summation is there to include particles on the terrace which have cascaded from odd to even sites before

diffusion, and the two terms before the summation are correction terms which must be included if $\alpha \neq 1/2$ or $\beta \neq 0$, respectively.

Using difference equation techniques,²² we have calculated the probability P_i that a particle deposited at site $2i$ (corresponding to a walker at site i in Fig. 2) will be absorbed at site 0, and we find the general expression

$$P_i = 1 - \frac{i}{c-1+R}, \quad (2)$$

where $R = (1-\gamma)/\gamma = (\nu_0/\nu_B)e^{E_B/k_B T}$. Substituting this equation with $c = (l-1)/2$ into Eq. (1) and replacing everywhere the terrace length l by $1/m$, we obtain the general expression for the surface current $J = J_1 + J_2$,

$$J = \frac{(2R-3) + m\{9 + 2R[2(\alpha+\beta) - 5]\}}{2[1 + (2R-3)m]}, \quad (3)$$

where $R = (\nu_0/\nu_B)e^{E_B/k_B T}$. As can be seen, our expression for the surface current depends on only two parameters: the downward funneling parameters α and β (which combine to form the combination $\alpha + \beta$) and the step-diffusion asymmetry ratio R . Given the assumptions used in our derivation, we expect this expression to be valid for m not too large (i.e., $m \leq 1/3$). We also note that in the above calculation, we ignored the possibility of islanding on a terrace. However, as long as the diffusion length σ is significantly longer than the terrace size $l = 1/m$, we expect Eq. (3) to be valid. This implies that as long as the selected slope is larger than $1/\sigma$, the existence of a finite diffusion length will not affect our estimate of the selected slope. However, for very small slope m (such that the terrace size is larger than the diffusion length) the surface current will be cut off by the diffusion length and will go to zero in the limit m goes to zero. The effect of a finite diffusion length on the existence of mounding at low temperature is discussed further below.

As can be seen from Eq. (3), for $R > 3/2$ the surface current is positive for small m leading to a mound instability, while for $R < 3/2$ the surface current is negative for small m and there is no mound formation. Thus there is a critical value of R ($R_c = 3/2$) required for mound formation. This implies that for a finite positive step barrier E_B , there exists a critical temperature above which mound formation does not occur. The critical value of R is independent of the parameters α and β which control the probability for an adatom deposited near a step edge to land on the upper or lower terrace since the effects of these parameters vanish in the limit of small slope m . We note that for the case of no step barrier ($E_B = 0$, $\nu_0 = \nu_B$) one has $R < R_c$ so that there is no mound instability, in agreement with simulations.¹⁶

From Eq. (3), we may obtain the selected mound slope as a function of R ,

$$m_0 = \frac{2R-3}{4R(1-\alpha-\beta) + 3(2R-3)} \quad (R \geq 3/2). \quad (4)$$

Equation (4) implies that as R approaches the critical value $R_c = 3/2$ from above, the mound slope decreases continuously to zero (for $\alpha + \beta < 1$). For $\alpha + \beta = 1$, the selected slope remains constant ($m_0 = 1/3$) for $R > 3/2$ and there is a discontinuous transition to zero mound angle at $R = 3/2$. We

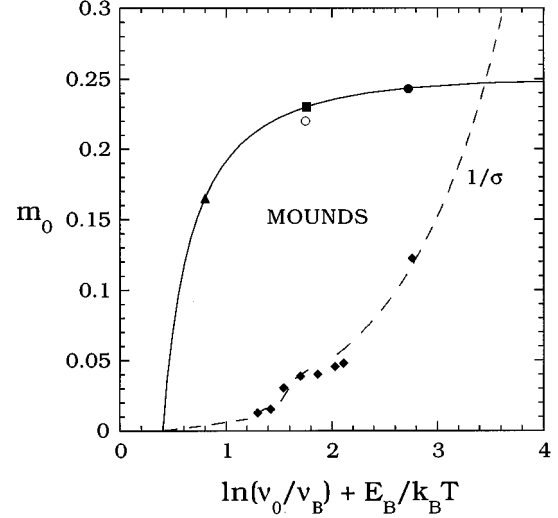


FIG. 3. Selected mound slope m_0 as a function of $r = \ln(\nu_0/\nu_B) + E_B/k_B T$ using Eq. (4) for the case $\alpha = 1/2$, $\beta = 0$ (solid line). Circles correspond to estimates obtained from simulations of Fe/Fe(100) deposition at room temperature in Ref. 15 (filled) and Ref. 17 (open). Square is experimental estimate (Ref. 11) while triangle is simulation result for a smaller value of r . Diamond-shaped symbols correspond to inverse diffusion length $1/\sigma$ for Fe/Fe(100) obtained from experimental results for the island density. The dashed line is a theoretical fit (see text).

note that for $\alpha + \beta > 1$, Eq. (4) implies a selected slope greater than $1/3$ so that Eqs. (3) and (4) may break down in this case. Therefore, in what follows, we restrict the discussion to the case $\alpha + \beta \leq 1$.

For the case of an infinite step-barrier ($R = \infty$), Eq. (4) implies $m_0 = 1/[5 - 2(\alpha + \beta)]$. For the case $\beta = 0$, this implies a maximum selected slope ranging from $m_0 = 1/5$ for $\alpha = 0$ (enhanced downward funneling) to $m_0 = 1/3$ for $\alpha = 1$ (enhanced upward funneling). For the case of an infinite step barrier with $\alpha = 1/2$ and $\beta = 0$ (corresponding to the usual downward funneling²³) we obtain $m_0 = 1/4$ in agreement with our previous calculation for this case.^{15,16} We note that this corresponds to a selected slope which is intermediate between that for a [103] facet and a [105] facet on a bcc(100) surface [or between a [113] facet and a [115] facet on a fcc(100) surface].

IV. RESULTS AND COMPARISON WITH EXPERIMENTS

Figure 3 shows the predicted mound slope using Eq. (4) as a function of $r = \ln R = \ln(\nu_0/\nu_B) + E_B/k_B T$ for the case $\alpha = 1/2$ and $\beta = 0$ (corresponding to the usual downward funneling²³). For $r > 1$ the selected mound slope is very close to the infinite barrier value $m_0 = 0.25$, so that the selected mound angle is essentially independent of temperature over this range. However, for $r < 1$ there is a very rapid decrease in the mound slope, with a critical value for mound formation corresponding to $r_c = \ln(3/2) \approx 0.405$. Also shown in Fig. 3 are the estimated mound slopes obtained from room temperature kinetic Monte Carlo simulations of the surface current using different values of r along with the experimental estimate for Fe/Fe(100) deposition at room temperature ($m_0 = 0.23$) which corresponds, assuming $\alpha = 1/2$, $\beta = 0$, to

$r \approx 1.8$. As can be seen, there is very good agreement between the simulation results and Eq. (4). We note that the $r \approx 2.7$ estimate ($m_0 \approx 0.24$) corresponds to simulations of Fe/Fe(100) deposition with $\nu_0/\nu_B = 1$ and an estimated step barrier $E_B = 0.07$ eV.¹⁵ The $r \approx 1.7$ estimate ($m_0 \approx 0.22$) corresponds to an estimate for the mound angle for Fe/Fe(100) (Ref. 17) made using a smaller value for the step barrier ($E_B = 0.045$ eV) obtained assuming infinitely fast edge diffusion.

We note that the condition for mound formation $r > r_c$ implies that if $E_B > 0$, then if $\nu_0/\nu_B < 3/2$ there exists a critical temperature for mound formation which is independent of α and β , i.e.,

$$T_c = \frac{E_B/k_B}{\ln(3/2) - \ln(\nu_0/\nu_B)}. \quad (5)$$

For $T > T_c$ mound formation does not occur. Since detachment from step edges may lead to a significant reduction in the upward current at high temperature, this is most likely an upper bound for T_c . However, if $E_B > 0$ and $\nu_0/\nu_B > 3/2$, then (neglecting the reduction in the surface current due to step detachment or island formation) mound formation occurs at all temperatures and there is no critical temperature for mound formation. On the other hand, if $E_B < 0$ (negative step barrier) and $\nu_0/\nu_B > 3/2$, then Eq. (5) implies a lower critical temperature for mound formation such that there is mound formation for $T > T_c$ but not for $T < T_c$. Finally, if $E_B < 0$ and $\nu_0/\nu_B < 3/2$, then there is no mound formation at any temperature and one expects logarithmic, quasi-layer-by-layer growth.^{16,25} For the case of no step barrier ($E_B = 0$) the critical value of ν_0/ν_B is equal to $3/2$ for all temperatures. Figure 4 shows a plot of the critical temperature for mound formation as a function of the ratio ν_0/ν_B for both $E_B > 0$ and $E_B < 0$.

Assuming $\nu_0/\nu_B = 1$ along with the estimates of the step barrier for Fe/Fe(100) obtained in Ref. 15 ($E_B = 0.07$ eV) and Ref. 24 ($E_B = 0.045$ eV) we obtain a value ($T_c^{\text{est}} = 1300 - 1800$ K) which most likely overestimates T_c for Fe/Fe(100). In particular, quasi-layer-by-layer growth for Fe/Fe(100) has been observed near $T = 800$ K.^{12,26} However, if $\nu_0/\nu_B = 0.7$, this leads (along with a slight reduction in the estimated step barriers) to a large reduction in the estimated critical temperature ($T_c^{\text{est}} = 500 - 900$ K). Thus, the estimated critical temperature for mound formation depends sensitively on the ratio ν_0/ν_B as well as on the step barrier.

As already noted, in our calculation of the surface current J we have ignored interactions between adatoms and existing islands or other adatoms. As long as the selected terrace size is less than the diffusion length σ (e.g., $m_0 > 1/\sigma$, where σ is in units of half the distance between fourfold hollow sites) then this interaction may be ignored. However, when the average terrace size is greater than or equal to σ (e.g., $m_0 \leq 1/\sigma$) then the surface current may be modified by the presence of islands. In order to see if this is the case for Fe/Fe(100) deposition, we have also included in Fig. 3 an estimate of $1/\sigma$ obtained using experimental results for the island density (per site) N at 0.07 ML coverage^{26,27} via the formula $1/\sigma \approx 3^{1/4} \sqrt{3N/2}$. Here we have assumed a regular triangular array of islands and σ has been taken to be equal to one-half the distance between an island and the center of

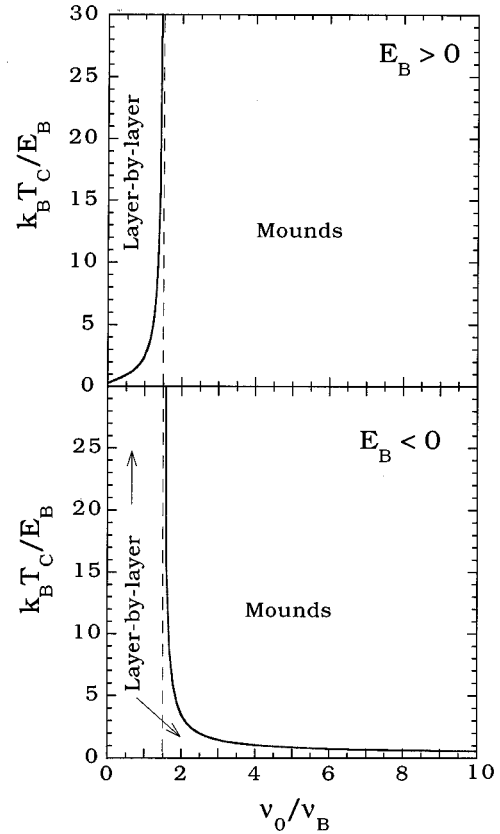


FIG. 4. Critical temperature T_c for mound formation predicted by Eq. (5) as a function of the prefactor ratio ν_0/ν_B for both positive and negative step barrier.

each triangle. (The value of r has been estimated assuming $\nu_0/\nu_B = 1$ and $E_B = 0.07$ eV.) Also shown is a theoretical fit²⁸ for $1/\sigma$ (dashed line) which extends to both lower and higher temperatures the estimates based on the experimental island density. As can be seen, at high temperatures (small $E_B/k_B T$) the diffusion length increases quite rapidly so that $1/\sigma \ll m_0$ and the average terrace size remains significantly larger than the diffusion length. Accordingly, the existence of mounds in Fe/Fe(100) does not appear to be affected by the diffusion length at high temperature. However, at low temperature (large $E_B/k_B T$) the diffusion length becomes significantly smaller than the selected terrace size and in fact eventually becomes smaller than a lattice constant. This leads to the suppression of mounding for $E_B/k_B T > 3.4$ and reentrant logarithmic growth of the surface width. This is consistent with simulation results at finite temperature ($T = 213$ K corresponding to $E_B/k_B T = 3.5$ with $E_B = 0.07$ eV) (Ref. 16) in which a constantly decreasing ‘‘mound angle’’ and quasilogarithmic growth of the surface width was observed. The behavior in the very low temperature limit in which there is no diffusion has already been discussed in Refs. 15, 23, and 24.

V. CONCLUSIONS

We have calculated the selected mound angle for growth on bcc(100) and fcc(100) surfaces for the case of a finite step barrier E_B , using a quasi-one-dimensional model with

irreversible attachment at up-steps and a variable probability for downward funneling of atoms landing near a step edge. For the case of an infinite step barrier (with $\beta=0$) we found that the selected slope varies between $m_0=1/5$ for $\alpha=0$ (corresponding to enhanced downward funneling at a step edge) and $m_0=1/3$ for $\alpha=1$ (enhanced upward funneling at a step edge). We note that the first case ($m_0=1/5$) is consistent with experiments on Cu/Cu(100) at 200 K in which [115] facets were observed while the second case ($m_0=1/3$) is consistent with experiments on Cu/Cu(100) at 160 K in which [113] facets were observed. For the case of an infinite barrier with $\alpha=1/2$ and $\beta=0$ (corresponding to the usual downward funneling²³) we find $m_0=1/4$ in good agreement with a recent calculation and simulations for this case. For all $\alpha+\beta\leq 1$ we find that there exists a critical value of the parameter $r=\ln(\nu_0/\nu_B)+E_B/k_B T$ [$r_c=\ln(3/2)\approx 0.405$] such that for $r<r_c$ mound formation no longer occurs. For $E_B>0$ and $\nu_0/\nu_B<3/2$ this implies the existence of a critical temperature for mound formation above which mounds are not formed, while for $E_B>0$ and $\nu_0/\nu_B>3/2$ no critical temperature for mound formation is predicted. For $E_B<0$ and $\nu_0/\nu_B>3/2$ this implies the existence of a lower critical temperature for mound formation while for $E_B<0$ and $\nu_0/\nu_B<3/2$ quasilogarithmic growth of the surface width is expected at all temperatures.

We have also presented extensive numerical and simulation results for the case of a finite step barrier E_B with $\alpha=1/2$ and $\beta=0$. In this case we find that for a sufficiently large value of the step barrier, e.g., $r=\ln(\nu_0/\nu_B)+E_B/k_B T>1$, the selected mound angle is relatively indepen-

dent of temperature. These results appear to explain the relatively good agreement for the mound angle obtained between recent simulations assuming different values for the step barrier E_B and also the good agreement with Fe/Fe(100) experiments. Furthermore, our analytical results account essentially quantitatively for the observed experimental and simulation results for Fe/Fe(100) at room temperature. While our results appear to overestimate the critical temperature for mound formation in Fe/Fe(100), we have shown that inclusion of a number of likely effects (such as $\nu_0/\nu_B\neq 1$ or the inclusion of detachment from step edges at high temperatures) may account for this overestimate. Finally, we have considered the effects of a finite diffusion length on the existence of mounds. In particular, we have shown that for Fe/Fe(100) at high temperatures the diffusion length remains higher than the selected terrace size and therefore the finite diffusion length does not affect mound formation. However, as the temperature is decreased the diffusion length becomes significantly shorter than the predicted terrace size leading to reentrant behavior as has been observed in simulations at low temperature^{16,23,24} and in experiments.^{29,30}

ACKNOWLEDGMENTS

This work was supported by National Science Foundation Grant No. DMR-9520842 and by the Office of Naval Research. Part of this work was carried out using the computational facilities of the Cherry L. Emerson Center for Scientific Computation at Emory University.

-
- ¹G. Ehrlich and F. Hudda, J. Chem. Phys. **44**, 1039 (1966); R.L. Schwoebel, J. Appl. Phys. **40**, 614 (1969).
- ²G. Rosenfeld, R. Servanty, Ch. Teichert, B. Poelsema, and G. Comsa, Phys. Rev. Lett. **71**, 895 (1993).
- ³J. Tersoff, A.W. Denier van der Gon, and R.M. Tromp, Phys. Rev. Lett. **72**, 266 (1994).
- ⁴K. Bromann, H. Brune, H. Roder, and K. Kern, Phys. Rev. Lett. **75**, 677 (1995).
- ⁵J. Villain, J. Phys. I (France) **1**, 19 (1991).
- ⁶M.D. Johnson, C. Orme, A.W. Hunt, D. Graff, J. Sudijono, L.M. Sander, and B.G. Orr, Phys. Rev. Lett. **72**, 116 (1994); C. Orme, M.D. Johnson, J. Sudijono, K.T. Leung, and B.G. Orr, Appl. Phys. Lett. **64**, 860 (1994).
- ⁷G.W. Smith, A.J. Pidduck, C.R. Whitehouse, J.L. Glasper, and J. Spowart, J. Cryst. Growth **127**, 966 (1993).
- ⁸M. Albrecht, H. Fritzsche, and U. Gradmann, Surf. Sci. **294**, 1 (1993).
- ⁹K. Fang, T.-M. Lu, and G.-C. Wang, Phys. Rev. B **49**, 8331 (1994).
- ¹⁰H.-J. Ernst, F. Fabre, R. Folkerts, and J. Lapujoulade, Phys. Rev. Lett. **72**, 112 (1994).
- ¹¹J.A. Stroschio, D.T. Pierce, M. Stiles, A. Zangwill, and L.M. Sander, Phys. Rev. Lett. **75**, 4246 (1995).
- ¹²K. Thürmer, R. Koch, M. Weber, and K.H. Rieder, Phys. Rev. Lett. **75**, 1767 (1995).
- ¹³J.E. Van Nostrand, S. Jay Chey, M.-A. Hasan, D.G. Cahill, and J.E. Greene, Phys. Rev. Lett. **74**, 1127 (1995).
- ¹⁴W.C. Elliott, P.F. Miceli, T. Tse, and P.W. Stephens (unpublished).
- ¹⁵F. Family and J. G. Amar, in *Evolution of Epitaxial Structure and Morphology*, edited by A. Zangwill, R. Clarke, D. Jesson, and D. Chambliss, Materials Research Society Symposia Proceedings No. 399 (MRS, Pittsburgh, 1996), p. 67; J. G. Amar and F. Family, Phys. Rev. B (to be published).
- ¹⁶J.G. Amar and F. Family, Surf. Sci. **365**, 177 (1996).
- ¹⁷M.C. Bartelt and J.W. Evans, in *Evolution of Epitaxial Structure and Morphology* (Ref. 15).
- ¹⁸M. Siegert and M. Plischke, Phys. Rev. Lett. **73**, 1517 (1994).
- ¹⁹J. Krug, M. Plischke, and M. Siegert, Phys. Rev. Lett. **70**, 3271 (1993).
- ²⁰P. Smilauer and D.D. Vvedensky, Phys. Rev. B **52**, 14 263 (1995).
- ²¹M. Siegert and M. Plischke, Phys. Rev. E **53**, 307 (1996).
- ²²H. Tuckwell, *Elementary Applications of Probability Theory* (Chapman and Hall, New York, 1988).
- ²³J.W. Evans, D.E. Sanders, P.A. Thiel, and A.E. DePristo, Phys. Rev. B **41**, 5410 (1990); H.C. Kang and J.W. Evans, Surf. Sci. **271**, 321 (1992).
- ²⁴M.C. Bartelt and J.W. Evans, Phys. Rev. Lett. **75**, 4250 (1995).
- ²⁵S.F. Edwards and D.R. Wilkinson, Proc. R. Soc. London Ser. A **381**, 17 (1982).
- ²⁶J.A. Stroschio, D.T. Pierce, and R.A. Dragoset, Phys. Rev. Lett. **70**, 3615 (1993); J.A. Stroschio and D.T. Pierce, Phys. Rev. B **49**, 8522 (1994).
- ²⁷J.G. Amar and F. Family, Phys. Rev. Lett. **74**, 2066 (1995).

²⁸In the theoretical fit we have used the experimental estimate for the terrace diffusion energy ($E_a=0.45$ eV). The theoretical fit also assumes a scaling of the form $N\sim(D/F)^{-\chi}$ for the island density (where D/F is the ratio of the terrace diffusion rate to the deposition rate) with $\chi\approx 1/3$ at low temperature (correspond-

ing to a critical island size $i=1$) and $\chi\approx 0.6$ at high temperature (corresponding to $i=3$) (Refs. 26 and 27).

²⁹W.F. Egelhoff, Jr. and I. Jacob, Phys. Rev. Lett. **62**, 921 (1989).

³⁰R. Kunkel, B. Poelsema, L.K. Verheij, and G. Comsa, Phys. Rev. Lett. **65**, 733 (1990).